Computer simulation of flow past superhydrophobic striped surfaces

Jiajia Zhou[1], Aleksey V. Belyaev[2,5], Evgeny S. Asmolov[2,3,4], Olga I. Vinogradova[2,5,6], and Friederike Schmid[1]

[1] Institut für Physik, Johannes Gutenberg-Universität Mainz,
Staudingerweg 7, D55099 Mainz, Germany
E-mail: {zhou, friederike.schmid}@uni-mainz.de

[2] A.N. Frumkin Institue of Physical Chemistry and Electrochemistry,
Russian Academy of Science, 31 Leninsky Prospect, 119991 Moscow, Russia

[3] Central Aero-Hydrodynamic Institute,
140180 Zhukovsky, Moscow region, Russia
[4] Institute of Mechanics, M.V. Lomonosov Moscow State University,
119991 Moscow, Russia

[5] Department of Physics, M.V. Lomonosov Moscow State University,
119991 Moscow, Russia
E-mail: oivinograd@yahoo.com

[6] DWI, RWTH Aachen,
Forckenbeckstraße 50, 52056 Aachen, Germany

We report results of Dissipative Particle Dynamics simulations for an anisotropic flow past superhydrophobic striped surfaces. We systematically vary several important parameters, such as the flow direction, the area fraction of the gas sectors, and the local slip length of the gas/liquid interface. We compare the simulation results with the numerical solution to the Navier-Stokes equations, analytic expressions, and asymptotic formulas in the limits where the local slip-length is small and large in comparison to the texture periodicity. The simulation results allow one to adjust surface properties to optimize transverse phenomena and passive microfluidic mixing. Our approach could be helpful to rational design of superhydrophobic surfaces.

1 Introduction

Fluid modeling from micrometer to nanometer scale not only is a fundamental problem in fluid mechanics, but also plays an important role in designing modern micro- and nanofluidic devices[1,2]. These devices have wide applications in different fields such as development of inkjet printheads for xerography, lab-on-a-chip technology, and most importantly, the manipulation and separation of DNA in molecular biology. Two assumptions which are often taken for granted in studies of macroscopic fluid phenomena, the no-slip boundary condition and the homogeneity of the surface, become doubtful in small length scales. The extension to partial-slip boundary condition and heterogeneous/anisotropic surfaces provide ample opportunities for simulations and applications.

Textured surfaces play a major role in microfluidics due to the high surface to volume ratio which greatly enhances the fluid-surface interaction. One example is the superhydrophobic Cassie surfaces, where no-slip area and partial-slip area arrange in a striped pattern. The partial-slip region consists of trapped gas, which is stabilized by a rough

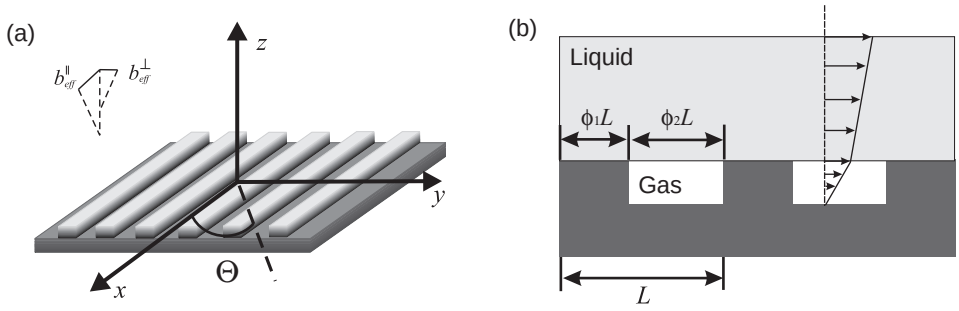

Figure 1: Sketch of the striped surface: $\Theta = 0$ to longitudinal stripes, $\Theta = \pi/2$ corresponds to transverse stripes (a), and of the liquid interface in the Cassie state (b).

wall texture and leads to a huge slip length[3] [see Fig. 1(a)]. These surfaces are known to be self-cleaning and causes droplets to roll (rather than slide) under gravity and rebound (rather than spread) upon impact. Besides that patterned superhydrophobic materials are important in context of fluid dynamics and their superlubricating properties. In particular, superhydrophobic heterogeneous surfaces in the Cassie state exhibit very low friction, and the resulting drag reduction is associated with the large slippage of liquids. Therefore, the ability to manipulate and control flow properties by varying the surface pattern has promoted interests to quantify the effects of surface heterogeneity and anisotropy.

In general it is difficult to quantify the flow past heterogeneous surfaces. However, analytical results can often be obtained by using an effective slip boundary condition, $\mathbf{b}_{\rm eff}$, at the imaginary smooth homogeneous, but generally anisotropic surface[4]. For an anisotropic texture, the effective slip depends on the direction of the flow and is a tensor, $\mathbf{b}_{\rm eff} \equiv \{b_{ij}^{\rm eff}\}$ represented by a symmetric, positive definite 2×2 matrix[5]

$$\mathbf{b}_{\rm eff} = \mathbf{S}_\Theta \begin{pmatrix} b_{\rm eff}^{\parallel} & 0 \\ 0 & b_{\rm eff}^{\perp} \end{pmatrix} \mathbf{S}_{-\Theta}, \tag{1}$$

diagonalized by a rotation

$$\mathbf{S}_\Theta = \begin{pmatrix} \cos\Theta & \sin\Theta \\ -\sin\Theta & \cos\Theta \end{pmatrix}. \tag{2}$$

The tensorial formalism allows one to calculate the effective slip in any direction given by an angle Θ, provided two eigenvalues of the slip-length tensor, $b_{\rm eff}^{\parallel}$ ($\Theta = 0$) and $b_{\rm eff}^{\perp}$ ($\Theta = \pi/2$), are known. For all anisotropic surfaces, the eigenvalues $b_{\rm eff}^{\parallel}$ and $b_{\rm eff}^{\perp}$ correspond to the fastest (greatest forward slip) and slowest (least forward slip) orthogonal directions.

In this report, we present Dissipative Particle Dynamics (DPD) simulations for a flow over superhydrophobic striped surfaces and compare our results with numerical solutions to Navier-Stokes equations[6,7] and some analytical theories[8–11].

2 Theory

We consider a creeping flow along a planar surface, and a Cartesian coordinate system (x, y, z) [Fig. 1(a)]. The origin of coordinates is placed at the flat interface. The local slip-length profile is alternating no-slip (area fraction ϕ_1) and partial slip (area fraction ϕ_2 and slip length b) regions, with the periodicity L [Fig. 1(b)]. Our system is based on the limit of a thick channel or a single interface, so that the velocity profile sufficiently far above the surface may be considered as a linear shear flow.

When the partial-slip region has a small slip length in comparison to the periodicity, $b \ll L$, it has been predicted that the effective slip-length tensor $\mathbf{b}_{\text{eff}}$ becomes isotropic, regardless of the type of surface textures[8,12],

$$b_{\text{eff}}^{\parallel,\perp} \simeq b\phi_2. \tag{3}$$

In the opposite limit where the gas sector becomes perfect slip, $b \gg L$, the eigenvalues of the effective slip-length tensor can be derived[13,14]

$$\frac{b_{\text{eff}}^{\parallel}}{L} = \frac{2b_{\text{eff}}^{\perp}}{L} \simeq \frac{1}{\pi} \ln\left[\sec\left(\frac{\pi\phi_2}{2}\right)\right]. \tag{4}$$

For more general cases of arbitrary value of b, Belyaev and Vinogradova[9] suggested approximate expressions for the effective slip,

$$\frac{b_{\text{eff}}^{\parallel}}{L} \simeq \frac{1}{\pi} \frac{\ln\left[\sec\left(\frac{\pi\phi_2}{2}\right)\right]}{1 + \frac{L}{\pi b} \ln\left[\sec\left(\frac{\pi\phi_2}{2}\right) + \tan\left(\frac{\pi\phi_2}{2}\right)\right]}, \tag{5}$$

$$\frac{b_{\text{eff}}^{\perp}}{L} \simeq \frac{1}{2\pi} \frac{\ln\left[\sec\left(\frac{\pi\phi_2}{2}\right)\right]}{1 + \frac{L}{2\pi b} \ln\left[\sec\left(\frac{\pi\phi_2}{2}\right) + \tan\left(\frac{\pi\phi_2}{2}\right)\right]}. \tag{6}$$

These formulas are accurate over large range of the parameters[9] and recover the right asymptotic in the large b limit [Eq. (4)].

A detailed analysis of the isotropic slip-length, Eq. (3), reveals that it can only apply for surfaces with a continuous slip profile[11], so its validity for the striped surface, which has step-like jump of the local slip at the stripe edges, is questionable. Recently, we derived a new asymptotic formula for weakly slipping surfaces ($b \ll L$),

$$\frac{b_{\text{eff}}^{\parallel}}{L} \simeq \varepsilon\phi_2 + \frac{2\varepsilon^2}{\pi}\left\{\ln\left[\frac{\pi\varepsilon}{\sin(\pi\phi_2)}\right] - \gamma\right\}, \tag{7}$$

$$\frac{b_{\text{eff}}^{\perp}}{L} \simeq \varepsilon\phi_2 + \frac{4\varepsilon^2}{\pi}\left\{\ln\left[\frac{2\pi\varepsilon}{\sin(\pi\phi_2)}\right] - \gamma\right\}, \tag{8}$$

where $\varepsilon = b/L$ and $\gamma = 0.5772157\ldots$ is Euler's constant.

3 Simulation Method

We apply Dissipative Particle Dynamics (DPD) method[15–17] to simulate the flow near striped superhydrophobic surfaces. The DPD method is an established coarse-grained, momentum-conserving method for mesoscale fluid simulations, which naturally includes thermal fluctuations. More specifically, we use a DPD version without conservative interactions[18]. The hydrodynamic boundary conditions are implemented using the tunable-slip method[19], which model the fluid-surface interaction using an effective friction force, combined with an appropriate thermostat.

The simulations are carried out using the open source simulation package ESPResSo[20]. Modifications have been made to incorporate the patterned surfaces. The simulation starts with randomly distributed particles inside the channel, and the flow is induced by applying a body force to all particles. A small body force is used to ensure the flow velocity near the wall is small, in order to avoid the effect of finite Reynolds number in simulations. The large system size leads to an increased simulation time (over 10^6 time steps) for the flow to reach a steady state. The flow velocity is small in comparison with the thermal fluctuation; thus the measurement also requires many time steps to obtain enough statistics. In this work, velocity profiles are averaged over 10^5 time steps. A fit to the plane Poiseuille flow then gives the effective slip length[7]. The error bars are obtained by six independent simulation runs with different initialization.

Based on the values of the velocities close to the surface, we estimate the characteristic Reynolds number of our system to be of $O(10)$, which is larger than those in real microfluidic devices. Thus, inertia effects may become important in simulations, and the Stokes equation is not strictly valid. This leads to a slight reduction of our simulation results for the effective slip in the transverse direction, but the flow in the longitudinal direction shall not be affected. To reach more realistic Reynolds numbers, we would need to reduce the body force by orders of magnitude. This would reduce the average flow velocity significantly, and the necessary simulation time to gather data with sufficiently good statistics will then increase prohibitively.

4 Results and Discussion

In this section, we present DPD simulation results and compare them with numerical calculations and analytic formulas in section 2.

We start with varying Θ in a system where the no-slip and partial-slip areas are equal, $\phi_2 = 0.5$, and the slip length is in the intermediate region $b/L = 1.0$. Figure 2 shows the results for the effective downstream slip lengths, $b_{\text{eff}}^{(x)}$. Also shown are theoretical curves calculated using Eq. (1), which can be explicitly written as

$$b_{\text{eff}}^{(x)} = b_{\text{eff}}^{\parallel} \cos^2\Theta + b_{\text{eff}}^{\perp} \sin^2\Theta. \tag{9}$$

Here, the eigenvalues of the slip-length tensor are obtained by numerical method and from Eqs. (5,6). The simulation data are in good agreement with theoretical predictions, confirming the anisotropy of the flow and the validity of the concept of a tensorial slip for striped surfaces.

Next we examine the effect of varying the fraction of slippery gas/liquid interface, ϕ_2. Figure 3(a) shows the eigenvalues, $b_{\text{eff}}^{\parallel}$ and $b_{\text{eff}}^{\perp}$, of the slip-length tensor as a function of

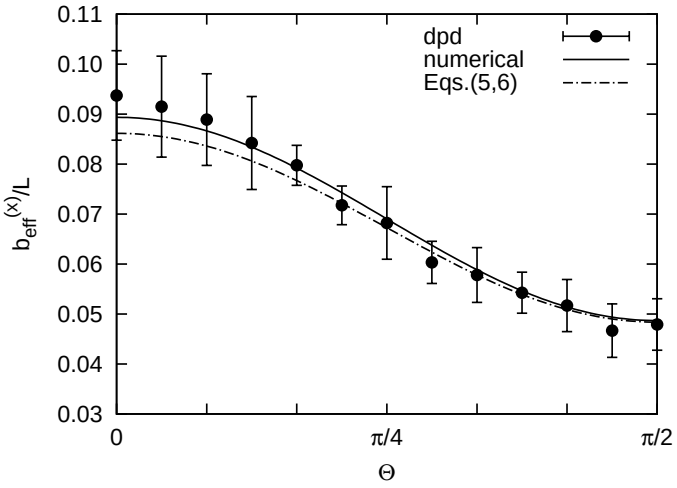

Figure 2: The effective downstream slip length, $b_{\rm eff}^{(x)}$, as a function of tilt angle Θ for a pattern with $b/L = 1.0$ and $\phi_2 = 0.5$. Symbols are simulation data. Curves are theoretical values calculated using Eq. (9) with eigenvalues obtained by a numerical method (solid) and by Eqs. (5,6) (dot-dashed).

ϕ_2, for a pattern with $b/L = 1.0$. The results clearly demonstrate that the gas fraction ϕ_2 is the main factor determining the value of effective slip, which significantly increases with the fraction of the slippery gas sectors. The theoretical curves match the simulation data very nicely.

We further examine the weakly slippery surfaces with $b/L = 0.034$ and present the longitudinal slip length $b_{\rm eff}^{\parallel}$ in Fig. 3(b). Here we compare several different theoretical predictions: the isotropic formula Eq. (3), the new asymptotic Eq. (7), and the analytical expression Eq. (5). The results for the transverse slip length $b_{\rm eff}^{\perp}$ are similar to those presented in Fig. 3(b), so we do not show them here. The values for the transverse component are smaller than those for the longitudinal component, indicating that the flow is anisotropic.

Finally, we present the eigenvalues of the effective slip-length tensor as a function of the slip length b at gas/liquid interface. The results for large values of b are shown in Fig. 4(a). The analytic formulas Eqs. (5,6) are shown in dot-dashed lines, which are accurate over large range of the b value. The effective slip lengths saturate when the slip length b is much greater than the stripe periodicity L, and reach the asymptotic values predicted by Eq. (4).

The simulation results and several theoretical predictions for small values of b are shown in Fig. 4(b). Again only the results for the longitudinal component is shown here, while the transverse component has a similar dependence. The surface-averaged slip, predicted by Eq. (3), is well above the exact values of the longitudinal effective slip. The analytical expressions Eq. (5), on the other hand, underestimates the effective slip. The newly developed formulas, Eq. (7), on the other hand, gives the correct asymptotic behavior in the limit of very small b/L.

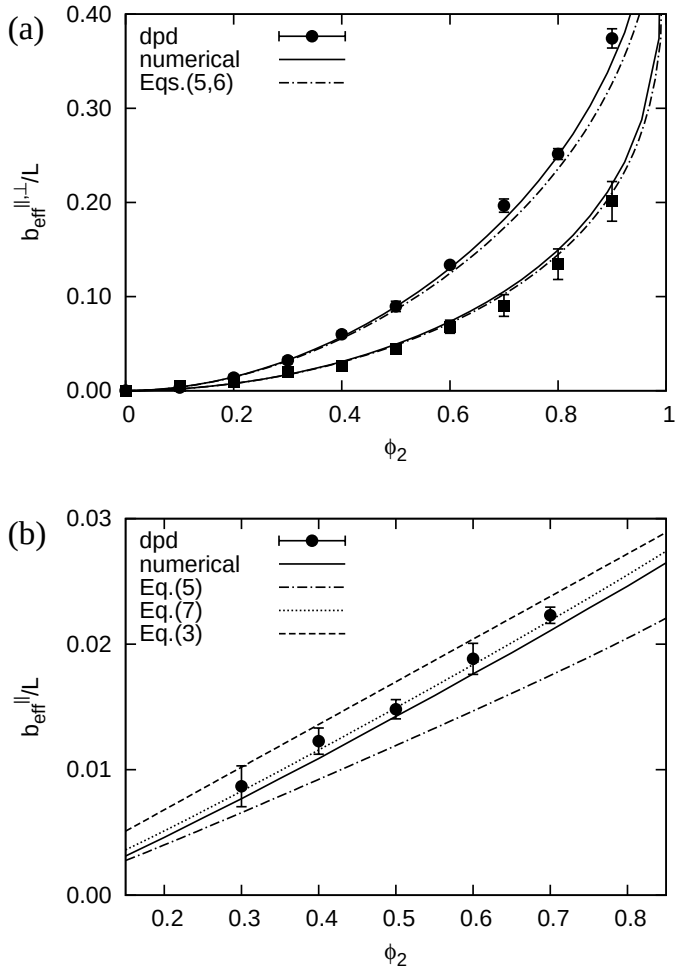

Figure 3: The eigenvalues of the effective slip-length tensor (symbols) as a function of gas-sector fraction ϕ_2 for (a) $b/L = 1.0$ and (b) $b/L = 0.034$. The numerical results are shown as solid curves. Also shown are asymptotic formulas Eq. (3) (dashed), Eq. (7) (dotted), and the analytic expressions Eqs. (5,6) (dot-dashed).

Acknowledgements

This research was supported by the DFG through SFB-TR6 and SFB 985, and by the RAS through its priority program "Assembly and Investigation of Macromolecular Structures of New Generations". The simulations were carried out using computational resources at the John von Neumann Institute for Computing (NIC Jülich).

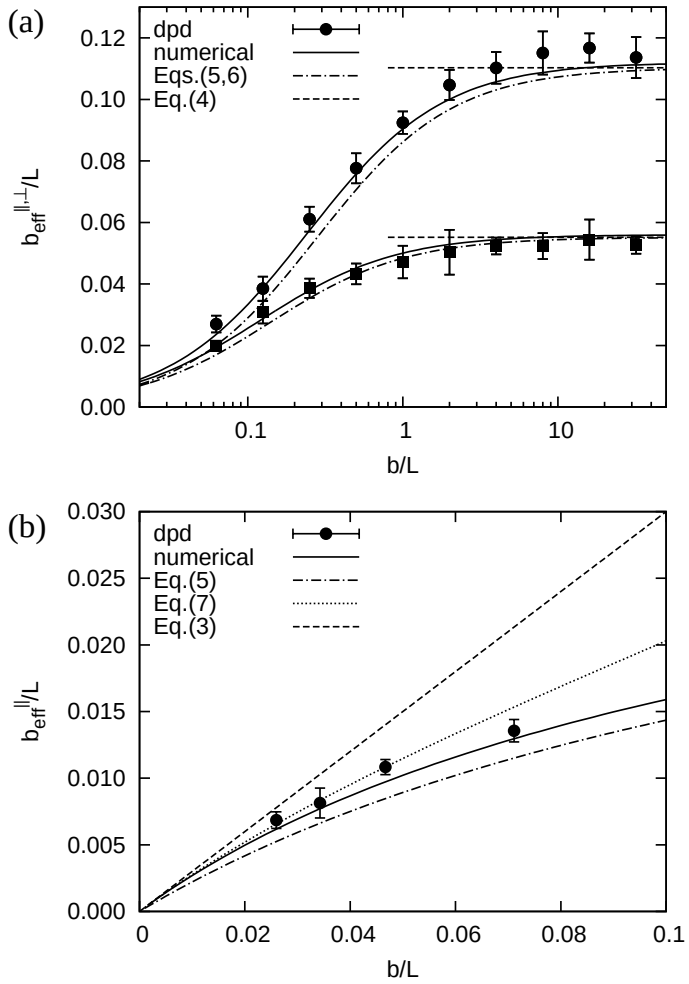

Figure 4: The eigenvalues of the effective slip-length tensor (symbols) as a function of local slip length b at the gas/liquid interface. The top figure (a) are results for large values of b and $\phi_2 = 0.5$, and the bottom figure (b) are results for weakly slipping surface and $\phi_2 = 0.3$. The numerical results are shown as solid curves. Also shown are asymptotic formulas Eqs. (3,4) (dashed), Eq. (7) (dotted), and the analytic expressions Eqs. (5,6) (dot-dashed).

References

1. H. A. Stone, A. D. Stroock, and A. Ajdari. Engineering flows in small devices: microfluidics toward a lab-on-a-chip. *Annu. Rev. Fluid Mech.*, 36:381, 2004.
2. T. M. Squires and S. R. Quake. Microfluidics: Fluid physics at the nanoliter scale. *Rev. Mod. Phys.*, 77:977, 2005.

3. David Quéré. Non-sticking drops. *Rep. Prog. Phys.*, 68:2495, 2005.
4. O. I. Vinogradova and A. V. Belyaev. Wetting, roughness and flow boundary conditions. *J. Phys.: Condens. Matter*, 23:184104, 2011.
5. M. Z. Bazant and O. I. Vinogradova. Tensorial hydrodynamic slip. *J. Fluid Mech.*, 613:125, 2008.
6. S. Schmieschek, A. V. Belyaev, J. Harting, and O. I. Vinogradova. Tensorial slip of superhydrophobic channels. *Phys. Rev. E*, 85:016324, 2012.
7. J. Zhou, A. V. Belyaev, F. Schmid, and O. I. Vinogradova. Anisotropic flow in striped superhydrophobic channels. *J. Chem. Phys.*, 136:194706, 2012.
8. K. Kamrin, M. Z. Bazant, and H. A. Stone. Effective slip boundary conditions for arbitrary periodic surfaces: the surface mobility tensor. *J. Fluid Mech.*, 658:409, 2010.
9. A. V. Belyaev and O. I. Vinogradova. Effective slip in pressure-driven flow past super-hydrophobic stripes. *J. Fluid Mech.*, 652:489, 2010.
10. E. S. Asmolov and O. I. Vinogradova. Effective slip boundary conditions for arbitrary onedimensional surfaces. *J. Fluid Mech.*, 706:108, 2012.
11. E. S. Asmolov, J. Zhou, F. Schmid, and O. I. Vinogradova. Effective slip-length tensor for a flow over weakly slipping stripes. *Phys. Rev. E*, 88:023004, 2013.
12. C. Ybert, C. Barentin, C. Cottin-Bizonne, P. Joseph, and L. Bocquet. Achieving large slip with superhydrophobic surfaces: Scaling laws for generic geometries. *Phys. Fluids*, 19:123601, 2007.
13. J. R. Philip. Flows satisfying mixed no-slip and no-shear conditions. *J. Appl. Math. Phys.*, 23:353, 1972.
14. E. Lauga and H. A. Stone. Effective slip in pressure-driven stokes flow. *J. Fluid Mech.*, 489:55, 2003.
15. P. J. Hoogerbrugge and J. M. V. A. Koelman. Simulating microscopic hydrodynamic phenomena with dissipative particle dynamics. *Europhys. Lett.*, 19:155, 1992.
16. P. Español and P. Warren. Statistical mechanics of dissipative particle dynamics. *Europhys. Lett.*, 30:191, 1995.
17. R. D. Groot and P. B. Warren. Dissipative particle dynamics: bridging the gap between atomistic and mesoscopic simulation. *J. Chem. Phys.*, 107:4423, 1997.
18. T. Soddemann, B. Dünweg, and K. Kremer. Dissipative particle dynamics: A useful thermostat for equilibrium and nonequilibrium molecular dynamics simulations. *Phys. Rev. E*, 68:046702, 2003.
19. J. Smiatek, M. Allen, and F. Schmid. Tunable-slip boundaries for coarse-grained simulations of fluid flow. *Eur. Phys. J. E*, 26:115, 2008.
20. H. J. Limbach, A. Arnold, B. A. Mann, and C. Holm. Espresso–an extensible simulation package for research on soft matter systems. *Comput. Phys. Commun.*, 174:704, 2006.